Int. J. Electrochem. Sci., 12 **(2017)** 8745 – 8760, doi: 10.20964/2017.09.33

International Journal of
ELECTROCHEMICAL
SCIENCE
www.electrochemsci.org

Azo Compounds as Green Corrosion Inhibitor for Carbon Steel in Hydrochloric Acid Solution: Corrosion Inhibition and Thermodynamic Parameters

A. S Fouda[1,*], *M. A. El-morsi*[2], *M. Gaber*[2], *M. Fakeeh*[3]

[1] Department of Chemistry, Faculty of Science, El-Mansoura University, El-Mansoura-35516, Egypt, Fax: +20502202271,Tel: +2 050 2365730
[2] Department of Chemistry, Faculty of Science, Tanta University
[3] Higher Institute of Engineering and Technology, New Damietta, Egypt
[*]E-mail: asfouda@hotmail.com
[*]E-mail: mfakeeh1985@gmail.com

Received: 28 April 2017 / *Accepted:* 30 June 2017 / *Published:* 13 August 2017

The influence of azo compound (L3) 2,4-dihydroxy-5-((5-mercapto-1H-1,2,4-triazol-3-yl)diazenyl)benzaldehyde) on the carbon steel (CS) corrosion in 1 M HCl was investigated using mass loss (ML), Tafel polarization (TP), electrochemical impedance spectroscopy (EIS) and electrochemical frequency modulation (EFM) tests. The protection efficiency (PE) improves with raising the concentration of inhibitor, but lesser with temperature rose. The inhibitor was adsorbed on the CS surface following Langmuir's adsorption isotherm. The electrochemical results showed that the investigated compound doing as mixed-kind inhibitor. Some thermodynamic parameters for activation and adsorption processes were determined and discussed. The inhibition mechanism was debated in the light of the chemical structure of the investigated compound.

Keywords: Corrosion protection; Carbon steel; HCl; Azo compounds; Adsorption isotherm

1. INTRODUCTION

CS is the extended metal utilized in industrial purpose, Army equipment, building and more in manufacturing of installations for petroleum, fertilizers and other industry. So the protection of C-steel in aqueous solutions is universal request, economic, environmental, and aesthetical important [1]. The use of inhibitor is more effective way to reduce the corrosion of CS. The organic assembled was commonly utilized as corrosion inhibitors as it contains heteroatom such as O, N, P, S, and heavy metals. But the organic compounds are hazards and unfriendly environment inhibitors [2-8], copper [9], aluminum [10-12], and other metals [13-17] in various corroding media. The surfactant adsorption by heterocyclic compounds on the surface of metal can markedly exchange the corrosion- resisting

assets of the metal [18-19] and so the revision of the relations among the adsorption and corrosion protection is of pronounced important. Heterocyclic compounds have exposed a good protection efficiency for iron in both HCl [20] and H_2SO_4 [21] solutions. There are growing concerns about certain compounds like chromates as inhibitors for corrosion processes, mainly due to the issue of toxicity. Greeninhibitors like natural products from plant extracts and substances from other renewable sources are of the interest of the researchers who are interested in "green chemistry" or "eco-friendly" technologies. The term "green inhibitor" or "eco-friendly inhibitor" refers to the substances that have biocompatibility in nature. The inhibitors like plant extracts presumably possess biocompatibility due to their biological origin. Similar to the general classification of "inhibitors", "green inhibitors" can also be grouped into two categories, namely organic green inhibitors and inorganic green inhibitors. Loto had reported the application of the extract of Mangifera indica leaves and bark for corrosion of mild steel in diluted H2SO4 medium [22,23]. The inhibitive effect of Zenthoxylum alatum fruit extract was reported for corrosion of mild steel in H_3PO_4 medium at temperatures ranging from 50–80^oC Satapathy et al studied the [24]. methanol extract of Justicia gendarussa leaves for corrosion inhibition of mild steel in HCl [25]. The inhibitive action of leaves, seeds and a combination of leaves and seeds of Phyllanthus amarus was reported by Okafor et al, for corrosion of mild steel in HCl and H2SO4 [26]. El-Etre investigated the stem extract of Opuntia for corrosion inhibition of Al in HCl solution [27]. Natural oils are one of the green inhibitors from plant sources. Pennyroyal oil was extracted from Mentha eulogium and studied for corrosion inhibition of steel in HCl solution [28]. Abdullah et al studied the inhibitory effect of natural clove oil for corrosion inhibition of nickel and its alloys namely, Inconel 600, and Inconel 690 in different concentrations of HCl solutions [29]. Ethuraman et al has performed a series of investigations on corrosion inhibition of mild steel in acidic medium using various plant extracts. For example, black pepper [30], Datura metel [31], and Strychnos nuxvomica [32] have been studied against the corrosion of mild steel in HCl as well in H2SO4. The extract of khillah seeds was studied against the corrosion of SX 316 stainless steel in HCl solution [33]. The anti-corrosion behavior of lupine, White lupine extract on the corrosion of steel in aqueous solution of H2SO4 and HCl was investigated by Abdel-Gaber et al [34]. Abiola et al described the inhibition of corrosion of Al in NaOH solution using leaves and seed extract of Gossipium hirsutum L [35]. The Gongronema latifolium extract was studied for corrosion inhibition of Al both HCl and NaOH solutions [36]. Corrosion inhibition of zinc in HCl solution was studied using Aloe vera gel extract [37].

The target of this research is to examine the corrosion performance of CS in 1 M HCl at various temperatures in the existence of azo compound utilized electrochemical and chemical tests. The CS morphology of the surface was estimated utilizing atomic force microscope (AFM) and FTIR analysis.

2. EXPERIMENTAL TESTS

2.1. Materials

Analysis of the CS coupons showed the presence of the following elements (wt %): 0.003 S, 0.20 C, 0.024 P, 0.350 Mn and the balance iron.

2.2. Solutions

The corrosive solution, 1 M HCl was prepared by dissolving of analytical mark (37 %) HCl with second distilled water. The concentration range of the L3 utilized was $3x10^{-6}$-$18x10^{-6}$ M

2.3. Inhibitor

The investigated compound was selected from azo derivatives (L3), was prepared as before [38] and is shown as below:

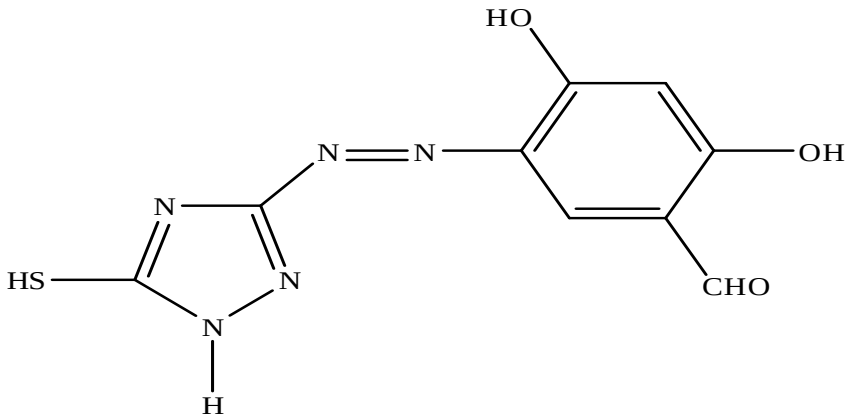

2,4-dihydroxy-5-((5-mercapto-1H-1,2,4-triazol-3-yl) diazenyl) benzaldehyde) (L3) $C_9H_7N_5O_3S$ **Mol. Wt.:** 265.25

2.4. Mass loss (ML) measurements

Seven similar CS pieces of 25 × 20 × 0.2 mm were scraped with emery paper (size 400–600–1300). After exact massing, the coins were deep beaker, which confined 250 ml of HCl with and without various concentrations of examined L3. All the corrosive solutions were air exposed. After 3 h, the coins were taken out and weighed exactly. The average ML of the seven similar CS was obtained. The % PE and θ, of azo (L3) compound were computed as next [39]:

$$\% PE = \theta \, x \, 100 = [1 - (W / W^{\circ})] \times 100 \quad (1)$$

Where W and Wº are the average mass losses with and without L3, respectively.

2.5. Electrochemical tests

TP tests were done in a square 3 electrode cell with electrode Pt and (SCE) as reference. The working electrode (1 cm^2) was a CS sheet surrounded by epoxy resin. TP diagrams were given by exchanging the potential of electrode spontaneously from -1.0 to 0.1 V with scan rate 1 mV s^{-1}. Stern-Geary tests [40] utilized for the purpose of calculation of current and potential of corrosion, then i_{corr} was utilized for measure of (θ) and % PE as next:

$$\% PE = \theta \, x \, 100 = [1 - (i_{(inh)} / i_{(free)}] \times 100 \quad (2)$$

Where $i_{(free)}$ and $i_{(inh)}$ are the currents in nonexistence and existence of L3, respectively.

EIS tests were take place by AC signals at OCP. The leading parameters given from the study of Nyquist diagram are R_{ct} (diameter of high frequency loop) and the double layer capacitance (C_{dl}) is given from:

$$C_{dl} = 1/ 2 \pi f_{max} R_{ct} \quad (3)$$

The PE and (θ) obtained from the EIS were distinct by:

$$\% PE = 100 x \theta = 100 \times \left[1 - \left(\frac{R^{\circ}_{ct}}{R_{ct}}\right)\right] \quad (4)$$

Where R_{ct} and R^{o}_{ct} are the charge transfer resistances in the absence and presence of L3, respectively.

EFM can be used as a rapid and noncorrosive technique for corrosion rate measurements without prior knowledge of Tafel constants. EFM carried out using two frequencies 2.0 and 5.0 Hz. The base frequency was 0.1 Hz. In this study, we use a perturbation signal with amplitude of 10 mV for both perturbation frequencies of 2.0 and 5.0 Hz. Equilibrium time leading to steady state of the specimens was 30 min. %PE was calculated using Eq. 2.

Calculations were done utilizing Gamry (PCI 300/4) Apparatus Galvanostat /Potentiostat /ZRA. This software contains a Gamry framework system established on the ESA 400. Gamry requests contain DC105 for corrosion tests. Echem software Analyst was utilized for graphing, plotting, and appropriate data.

2.6. Surface Analysis

The CS coins utilized for analysis of the surface morphology were abraded with various grades of scraping papers and immersed in the corrosive solution with and without $18x10^{-6}$ M of azo compound (L3) at room temperature for 1 day then tested by utilizing atomic force microscope (AFM) and FTIR.

3. RESULTS DATA AND DISCUSSION

3.1. Mass Loss tests

The time-ML plots of CS with in the aggressive medium at various concentrations of L3 are given in Figure 1.

The Figure 1 gives that the ML of CS is lowered in presence of various concentrations of L3 than in its absence, i.e., the PE increases with the presence of various concentrations of L3, this is record in the Table 1. This result trend may give the adsorption fact of L3 on the CS improve with the concentration of L3 thus the CS surface is efficiently separated from the medium by the formation of a layer of L3 on CS [41, 42].

Table 1. % PE and θ of L3 as function in various concentrations of L3 using ML tests at 120 min immersion time in 1 M HCl, 25°C

Conc., x 10^6 M	Θ	% PE
0.0	--	----
3	0.509	50.9
6	0.664	66.4
9	0.749	74.9
12	0.801	80.1
15	0.842	84.2
18	0.886	88.6

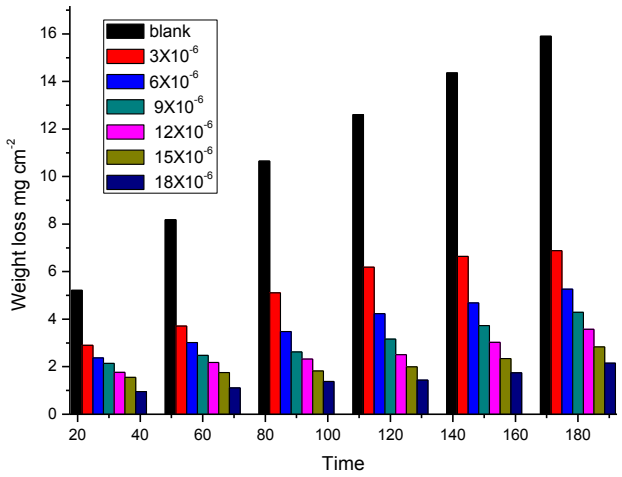

Figure 1. Time-ML plots for the CS corrosion with and without various concentrations of L3 at 25°C

3.2. TP tests

Figure 2 displays the cathodic and anodic plots in presence and absence of varying concentrations of L3 at 25°C.

From Figure 2, it was found that the anodic CS dissolution and cathodic H_2 loss were protect when examined L3 in 1.0 M HCl and this protection was more marked with improving concentrations of L3. Tafel slopes are moved to more potential positive and negative with esteem to the blank plots by improving the L3 concentration. This performance led to that the L3 acts as mixed type inhibitor [43]. The results showed that the increase in L3 concentration led to break down the current (i_{corr}) which led to the shift of the cathodic and anodic reactions slightly without varying the mechanism [44-46].

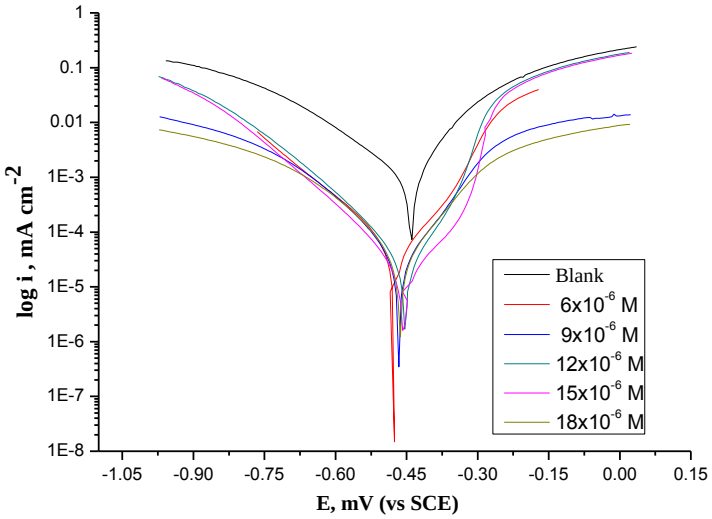

Figure 2. TP plots for CS corrosion in presence and absence of different concentrations of (L3) at 25 ºC

Table 2. TP values of CS corrosion with and without various concentrations of (L3) at 25°C

Conc., M	$-E_{corr}$, (mV vs SCE)	i_{corr}, µA cm^{-2}	$-\beta_c$, mV dec^{-1}	β_a, mV dec^{-1}	C.R mmy^{-1}	θ	% PE
Blank	471	181	173	79	82.8	------	-----
$6x10^{-6}$	464	45.4	156	122	20.6	0.749	74.9
$9x10^{-6}$	475	41.8	126	102	19.1	0.769	76.9
$12x10^{-6}$	466	34.2	128	103	15.6	0.811	81.1
$15x10^{-6}$	453	28.3	121	87	12.9	0.843	84.3
$18x10^{-6}$	456	21.8	128	128	9.9	0.879	87.9

3.3. EIS tests

The influence of L3 concentrations on the impedance performance of CS at 25ºC in with and without of various concentrations of L3 is shown in Figure 3 (a, b). The plots show a same kind of Nyquist diagrams for CS corrosion in the existence of various concentrations of L3. The appearance of semi-circle single give the single charge transfer procedure from dissolution. Examinations of the values given EIS curve contain of a maximum capacitive loop (Bode curves) (Figure 3b).

The equivalent electrical circuit is given in Figure 4. It utilized to examine the given EIS data. The typical include of the resistance solution (R_s), the charge-transfer (R_{ct}) and C_{dl}. Good typical was given with our examining value. EIS value (Table 3) give that the R_{ct} data raise and the data of C_{dl} lower with improving the concentration of L3. Because replacement of water molecules by the adsorption of L3 on the CS, decreasing the degree of dissolution reaction. The maximum (R_{ct}) data are commonly attendant with lower destroying system [47, 48]

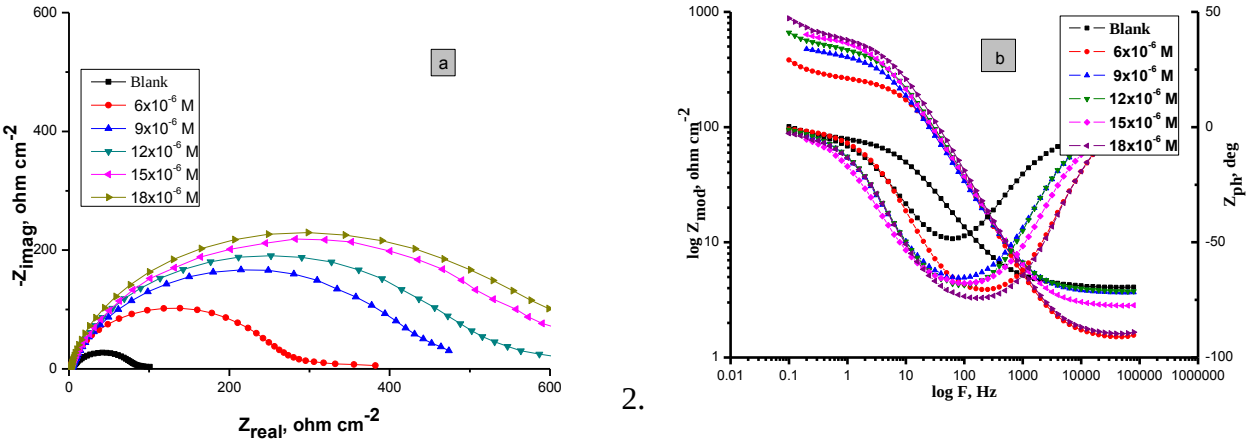

1. 2.

Figure 3. The Nyquist (a) and Bode (b) diagrams for corrosion of CS with and without various concentrations of L3 at 25°C

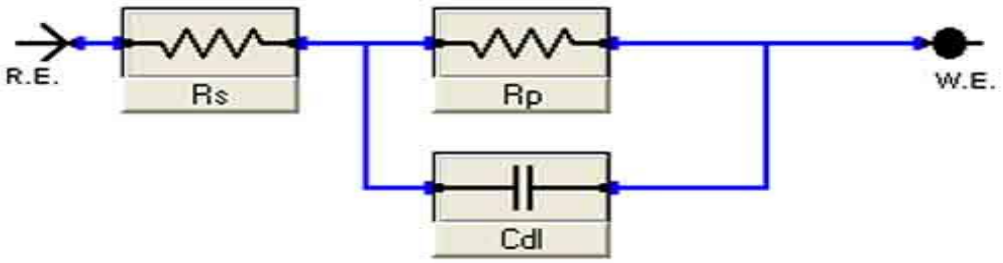

Figure 4. Equivalent electrical circuit utilized to fit the outcome of impedance

Table 3. EIS values of CS corrosion in 1 M HCl with and without various concentrations of L3 at 25°C

Concentration M	R_{ct}, Ω cm^2	C_{dl}, μF cm^{-2}	θ	% PE
Blank	83.5	7	-----	------
$6X10^{-6}$	279.4	5.6	0.701	70.1
$9X10^{-6}$	445.2	2.1	0.812	81.2
$12X10^{-6}$	523.5	1.6	0.840	84
$15X10^{-6}$	588.8	1.3	0.858	85.8
$18X10^{-6}$	638.4	1.1	0.869	86.9

The lower in the C_{dl} can give from lower of the local dielectric constant and/or from the improve of thickness of the electrical double layer proposed that the L3 molecules function by adsorption at the interface solution/metal [49].The % PE given from EIS calculation are nearly to those assumed from TP and ML calculations.

3.4. EFM tests

Table 4. Parameters given by EFM tests for CS corrosion with and without various concentrations of (L3) at 25°C

Conc., M	$i_{corr.}$, μA cm^{-2}	β_c, mV dec^{-1}	β_a, mV dec^{-1}	CF-2	CF-3	C.R, mmy^{-1}	Θ	% PE
Blank	225.8	91	69	1.9	2.8	103	------	------
$6x10^{-6}$	55.1	131	179	2.3	2.9	28	0.756	75.6
$9x10^{-6}$	39.2	123	188	1.9	3.0	19	0.826	82.6
$12x10^{-6}$	36.6	109	100	1.7	3.4	17	0.838	83.8
$15x10^{-6}$	35.7	103	96	1.6	3.2	16	0.842	84.2
$18x10^{-6}$	28.1	127	101	1.9	2.9	12	0.874	87.4

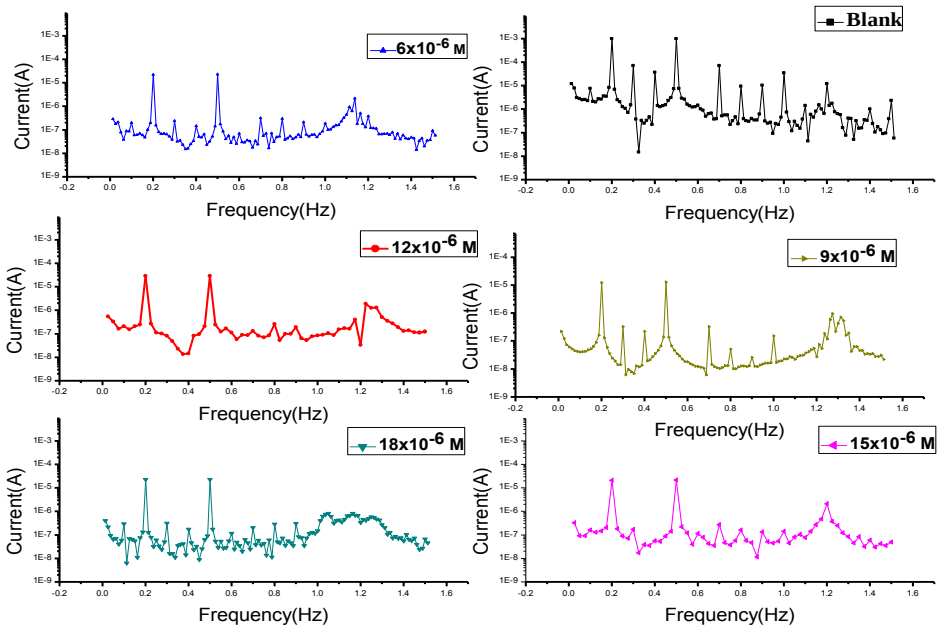

Figure 5. EFM for CS corrosion in the with and without of various concentrations of (L3)

The results of EFM tests are a spectrum of current reply as a function of frequency. The spectrum is named the intermodulation spectrum. The spectra include current responses consigned for harmonical and intermodulation current peaks. The rate of corrosion and Tafel slops can be given with one calculation by examining the harmonic frequencies. The maximum peaks were employed to

examine the causality factors, i_{corr}, β_c and β_a. Spectrum gives from EFM tests. As can be seen from Table (4), then i_{corr} was consequently given and utilized for examining the % PE and (θ) were measured from the equation 2. The causality factors CF2 & CF3 in Table (4) are very nearly too their theoretical values (2 &3) agreeing to the EFM theory [49]. The causality factors serve as internal check to the obtained results and their deviation from their ideal data (2&3) might due to that the amplitude of perturbation was too lower or that the frequency spectrum resolution is not enough high. Figures (5) represents the spectra of EFM for CS dissolution in with and without of various concentrations of (L3).

3.5. Adsorption isotherms

Organic compounds protect corrosion by the adsorption of L3 on surface of CS. In theory, the procedure can be observed as a single substitutional manner in which molecule of L3, I in the aqueous phase alternatives an "x" adsorbed on the CS [50,51]

$$xH_2O_{(sur)} + I_{(aq)} \longrightarrow xH_2O_{(aq)} + I_{(sur)} \quad (5)$$

where x is recognized as the bulk ratio and simply equals the number of adsorbed water molecules exchanged by a single L3. The adsorption influenced by nature of inhibitor. The data of θ for various concentrations of L3 at various temperatures have been utilized to elucidate the excellent isotherm to define the adsorption procedure. The results of examined L3 was good fitted by Langmuir isotherm. Figure 6 gives the diagram of C/θ versus C at 25°C for L3 inhibitor. This diagram gave straight lines signifying that the compound L3 adsorbed on CS surface obeying Langmuir isotherm [50]:

$$(C_{inh}/\theta) = (1/\ k_{ads}) + C_{inh} \quad (6)$$

where C = concentration ofL3 and K_{ads} = constant of adsorption associated to $\Delta G°_{ads}$ as [36]:

$$K_{ads} = 1/\ 55.5\ exp\ (-\Delta G°_{ads}/\ RT) \quad (7)$$

55.5 is the concentration of water in the bulk solution (mol/ l)

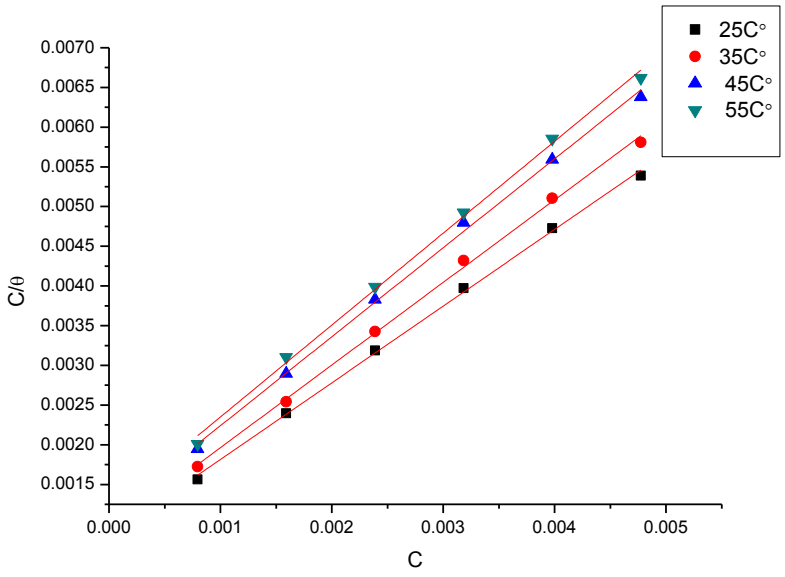

Figure 6. Langmuir plots for investigated L3 for the corrosion of CS in HCl solution at various temperatures

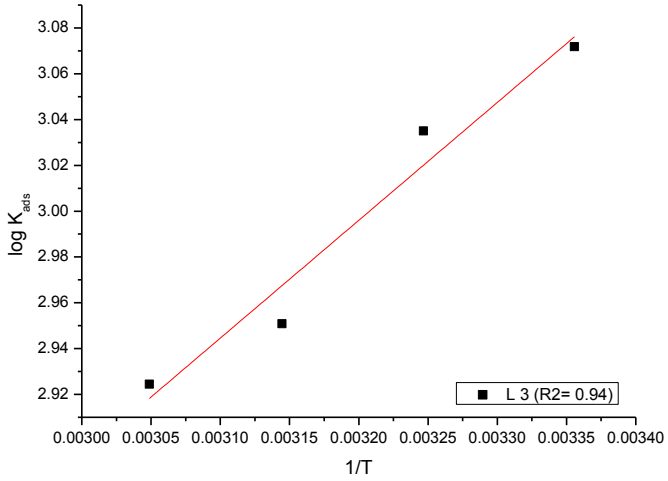

Figure 7. Log K_{ads} against 1/T for CS corrosion

Table 5. Adsorption parameters for the inhibitor L3 on CS surface at various temperatures

Temp. K	K_{ads}x 10^{-1} M^{-1}	$-\Delta G^{o}_{ads}$ kJ mol^{-1}	$-\Delta H^{o}_{ads}$ kJ mol^{-1}	$-\Delta S^{o}_{ads}$ J mol^{-1} K^{-1}
298	118	27.4	98.0	59.1
308	108	28.1		59.5
318	89	28.6		58.9
328	84	29.3		59.3

The values of K_{ads} and ΔG^{o}_{ads} for L3 were measured and are written in Table (5). All expected parameters for L3 on CS from molar HCl solution were record in Table (5). By analysis of the given values, it was creating that:

- The -ve values of $\Delta G°_{ads}$ return that the L3 adsorption on CS is spontaneous [52, 53].
- The increase of ΔG°_{ads} values (become fewer negative) with rise of temperature led to the existence of exothermic reaction at which adsorption was unfavorable as the outcome data of desorption of L3 from CS surface [53].

3.6 Temperature effect

The temperature effect on CS including various concentrations from examined inhibitor was measured by ML tests over a range of temperature from 25 to 55°C.The outcome data discovered that the rate of corrosion rises as the temperature improved and lowered as the concentration of L3 rises. The activation energy (E_a) of the corrosion of CS in HCl was measured utilized Arrhenius Equation:

$$k = A\ exp\ (-E_a / RT) \quad (8)$$

where A is the constant Arrhenius. Figure 8 shows the Arrhenius plots with and without various concentrations of L3. E_a data given from the slopes of these lines are record in Table 6. The

data of E_a for protected solution is upper than unprotected, signifying that dissolution of CS is lower in the attendance of L3 and can be deduced as due to physical adsorption [54]. It is recognized from Eq. 8 that the maximum E_a data lead to the lesser corrosion rate. Because founding a cover on the CS surface serving as an energy barrier for corrosion of CS [55].

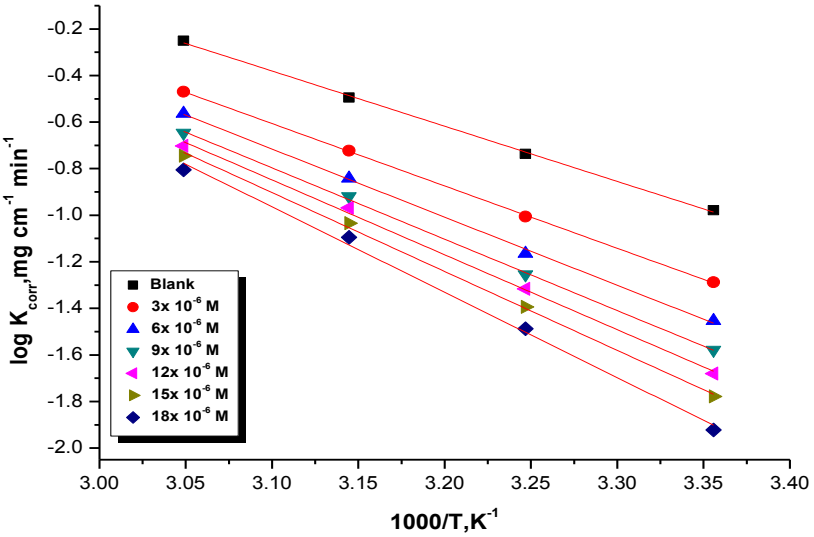

Figure 8. 1/T – Log k plots for CS corrosion in the with and without of various concentrations of *L3*

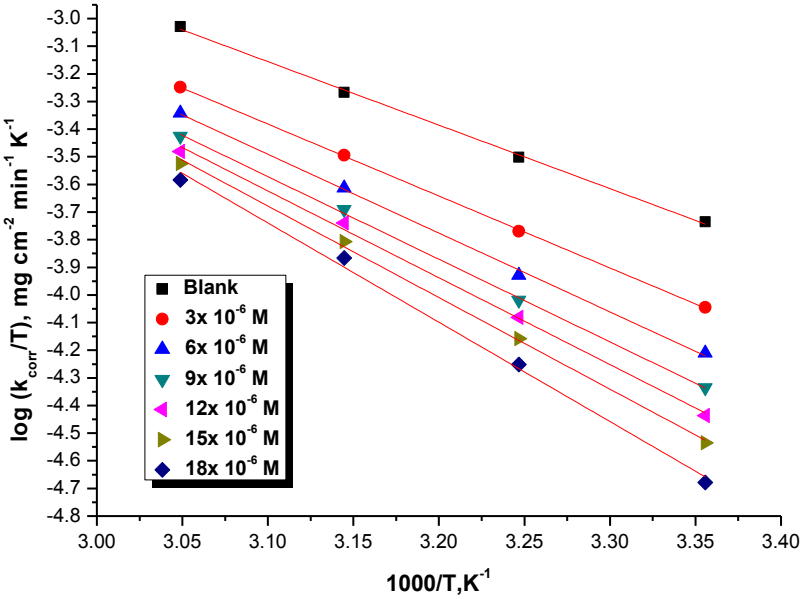

Figure 9. 1/T – Log k/T diagrams for CS dissolution in the with and without of various concentrations of L3

The thermodynamic parameters, ΔH^* and ΔS^*, of the corrosion process were calculated from the transition state equation Eq.9 and their values were recorded in Table 6

$$Rate = (RT/Nh)\, exp\,(\Delta S^*/R)\, exp\,(-\Delta H^*/RT) \quad (9)$$

where h is constant Planck's. A diagrams of log (Rate/ T) against 1/ T for CS in 1 M HCl at various concentrations of L3, obtain straight lines as displayed in Figure 9 for (L3). The +ve signs of ΔH^* redirect the endothermic type of the metal dissolution. Higher and -ve data of ΔS^* suggest that the activated complex in the rate-determining step prefers an association more than dissociation [56, 57].

Table 6. Parameters of CS corrosion of the investigated compound (L3)

Conc. M	$-E^*_a$ kJ mol^{-1}	ΔH^* kJ mol^{-1}	$-\Delta S^*$ J mol^{-1} K^{-1}
Blank	45	43	121
$3x10^{-6}$	51	49.	107
$6x10^{-6}$	55	54	95
$9x10^{-6}$	58	57	88
$12x10^{-6}$	61	60	80
$15x10^{-6}$	64	63	71
$18x10^{-6}$	70	68	55

3.7. AFM analysis

3. A

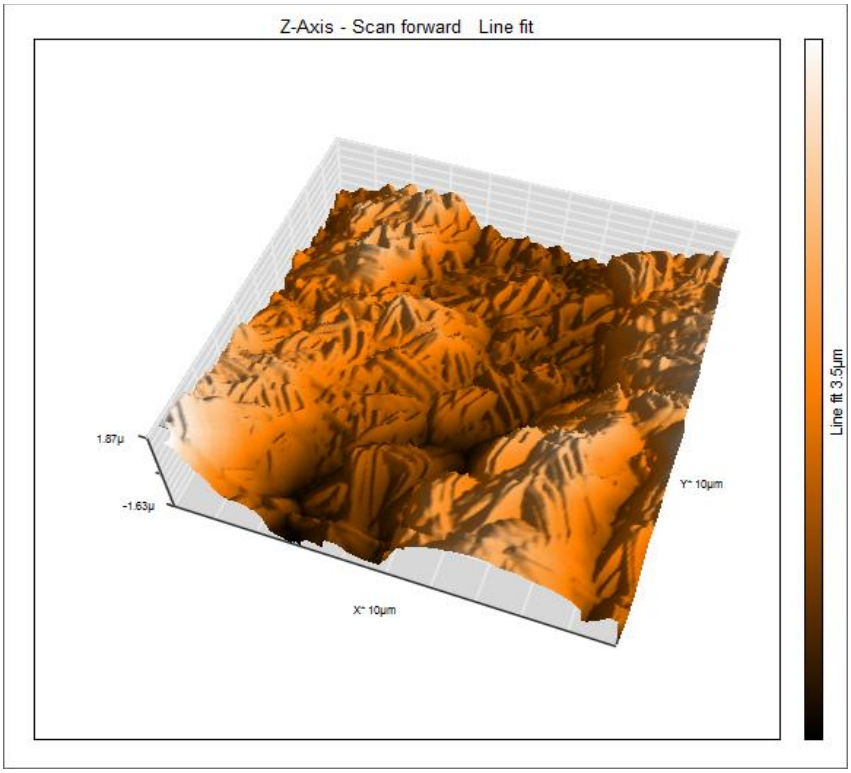

4.

5. B

6.

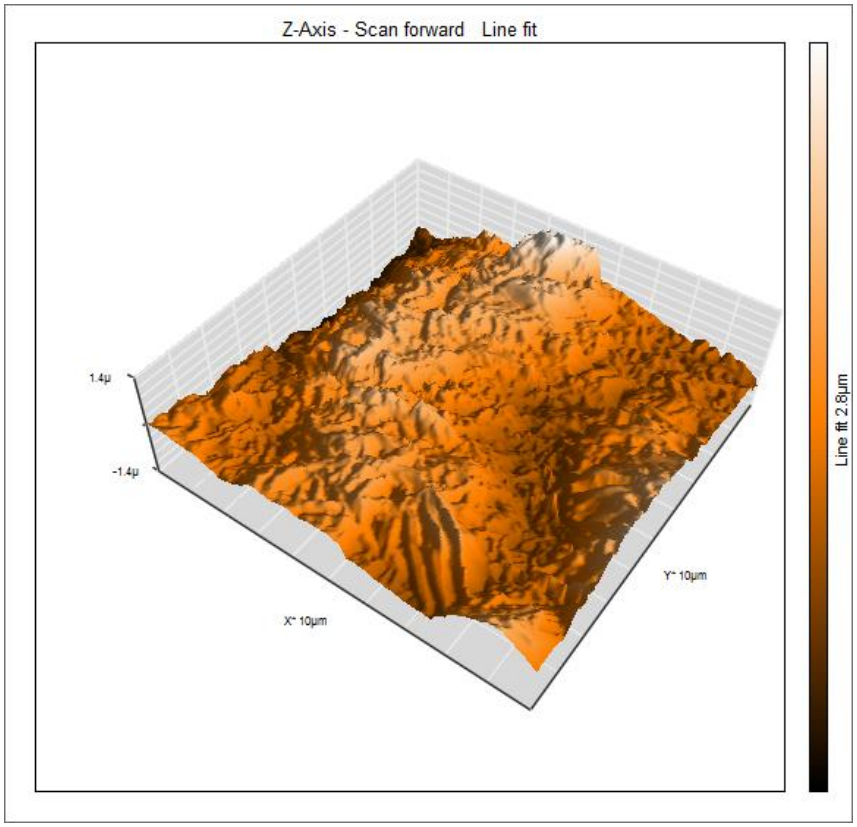

Figure 10. Three dimensional (3D) AFM images of the surface of: (a) Carbon steel immersed in 1 M HCl (blank) (b) Carbon steel immersed in 1 M HCl containing 18 x 10^{-6}M of inhibitor L3

AFM is a great test to examine the image of surface of different coins at nano-micro scale that is currently utilized to analyze the effect of corrosion inhibitor [58]. Examination of the images determines the roughness of surface over area scale of 5µm. The three dimensional AFM images of CS surface without and with inhibitor are shown in Fig. (10 a, b).The surface roughness of CS surface after immersion in 1 M HCl is up to 497 nm (Fig. 10a), while in the existence of inhibitor , the roughness lower to 289 nm (Fig. 10b). It shows that the CS surface in existence of L3 is more compact and uniform, so it can professionally protect CS surface from corrosion. This confirms that the protected surface is smoother than the uninhibited surface. The smoothness of the surface of CS is due to the development of a protective film on the CS surface.

3.7. FTIR analysis

Figures (11 a, b) represent the IR of L3 and that of the film created on the CS inundation in 1 M HCl, L3 (18x10^{-6}M). The FTIR spectrum of L3 solution free is shown Fig.11a. The -OH- stretching frequency at 3407 cm^{-1}, the -SH appears at 2307 $cm^{-1}$the C=O found at 1638 cm^{-1}, the -C=C at (1412 cm^{-1}) (multiple bands), the -CO obtain at 1148 $cm^{-1}$and the phenyl group with two function group in ortho position (-CHO and OH) appears at 744 cm^{-1}. The FTIR spectrum of solution after carbon steel

immersed in 1 HCl with L3 ($18x10^{-6}$M) is shown in Fig. 11b. The -SH moved from 2307 cm^{-1} to 2093 cm^{-1}, C=O stretching moved from 1638 cm^{-1} to 1646 cm^{-1}. The -C=C stretching, the -CO stretching and the phenyl group with two function group in ortho position are disappear [59].

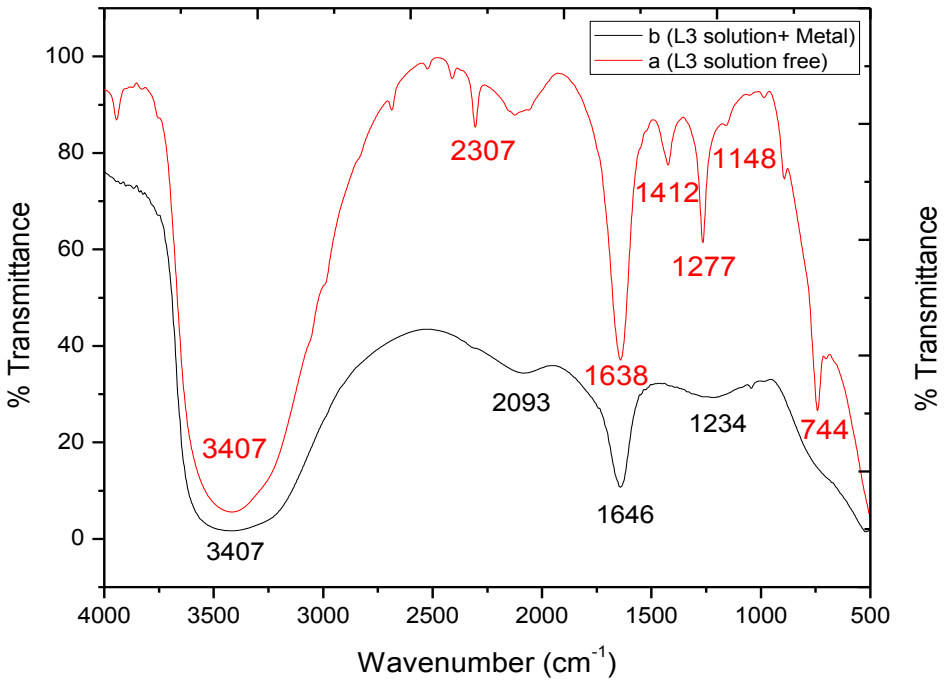

Figure 11. FTIR spectra of the film created on the CS surface in 1 M HCl, and in presence of L3 ($18x10^{-3}$M)

3.8. Mechanism of protection

Corrosion protection of CS by the examined azo compound 2,4-dihydroxy-5-((5-mercapto-1H-1,2,4-triazol-3-yl) diazenyl) benzaldehyde) (L3) from ML, EFM, EIS and TP tests was obtained and was found to rely on the concentration and the kind of the inhibitor. It is normally, presumed that the adsorption of the inhibitor at the interface solution / metal is the first step in the action mechanism of the inhibitor in HCl media. Four kind of adsorption may occurring during protection including organic atoms at the interface of solution / metal: Electrostatic attraction among charged metal and molecules, Interaction of unshared electrons pairs in the molecule with the carbon steel, Interface of π electrons with the CS, A mixture of the overhead [60]. Inhibitor concentration, the PE relies on numerous factors; such as number of adsorption center and their charge densities, hydrogenation heat, the founding metallic complexes and molecular size [61]. 2,4-dihydroxy-5-((5-mercapto-1H-1,2,4-triazol-3-yl) diazenyl) benzaldehyde) (L3) inhibitor includes a polar group with an atom of S, O, or N, each of them in principle demonstrating a chemisorptions center. The protective characteristic of such compound rely on the electron densities nearby the active center where the maximum electron density at the center the more effect the inhibitor.

4. CONCLUSIONS

Based on the experimental results the following conclusions can be drawn from the study:

The chemical and the electrochemical methods showed that (L3) is excellent corrosion inhibitor for the protection of CS in 1 M HCl. Tafel polarization results indicate a mixed inhibitor effect of (L3). (L3) was found to be physically adsorbed on the CS surface in HCl medium following Langmuir adsorption isotherm model. C_{dl} values decrease while R_{ct} values increase with the addition of different concentrations of (L3). AFM micrographs showed that CS surface was covered with a protective film of the (L3) inhibitor. All the studied techniques gave good agreement

References

1. M. Abdallah, B. A. AL Jahdaly, O. A. Al-Malyo, *Int. J. Electrochem. Sci*., 10 (2015) 2740.
2. M. Abdallah, A. M. El-Dafrawy, M. Sobhi, A. H. M. Elwahy, M. R. Shaaban, *Int. J. Electrochem. Sci.,* 9 (2014) 2186.
3. M. Sobhia, M. Abdallah, E. Hafez, *J. Advances in Chem*., 5 (2013) 830.
4. M. Abdallah, B. H. Asghar, I. Zaafarany, M. Sobhi, *Protection Metals and Phys Chem. of Surfaces*, 49 (2013) 485.
5. A. S. Fouda, M. Abdallah and M. Medhat, *Protection Metals and Phys Chem. of Surfaces*, 48 (2012) 477.
6. S. Issaadi, T.Douadi, A. Zaouaoui, S. Chafaa, M. A. Khan, G. Bouet, *Corros. Sci*., 53 (2011) 1484.
7. M. Abdallah, I. Zaafarany, K. S. Khairou, M. Sobhi, *Int. J. Electrochem Sci*., 7(2012)1564.
8. A. S. Fouda, S. A. El-Sayyed, M. Abdallah, *Anti-Corrosion Methods and Materials*, 58 (2011) 63.
9. G. Moretti, F. Guidi, F.Fabris, *Corros. Sci*., 76 (2013) 206.
10. A. S.Fouda, M. Abdallah, A. Attia, *Chem.Engineering Comm*., 197 (2010) 1091.
11. M.Abdallah, H. E. Megahed, M. S. Motae, *Mater. Chem. Phys*., 118 (2009) 111.
12. M. Abdallah, M. E. Moustafa, *Annali Di Chimica*, 94 (2004) 601.
13. F. Bentiss, M. Lagrrene, M. Traisnel, *Corrosion*, 56 (2000)733.
14. M. Abdallah, E. A. Helal, A. S. Fouda, *Corros. Sci*., 48 (2006) 1639.
15. G. Moretti, F. Guide, G. Grion, *Corros. Sci*., 46 (2004) 387-395.
16. E. S. Ferreira, C. Giancomelli, F. C. Giacomelli, A. Spinelli, *Mater. Chem. Phys*., 83(2004) 129.
17. M. S. Morad, *Corros. Sci*., 50 (2008) 436.
18. F. BentissTraisnel, M. Lagrene, *Corros.Sci.,* 42 (2000) 127.
19. M. A. B. Christopher, A. R. G. Isabel Jenny, *Corros.Sci.*, 36 (1994) 915.
20. M. Elachouri, M. S. Hajji, M. Salem, S. Kertit, J. Aride, R. Coudert, E. Essassi, *Corrosion*, 52 (1996) 103.
21. A. S. Algaber, E. M. El-Nemma, M. M. Saleh, *Mater.Chem.Phys,* 86 (2004) 26.
22. C. A. Loto, *Corros. Prev. Cont.*, 48 (2001) 38.
23. C. A Loto, *Corros. Prev. Cont.*, 48 (2001) 59.
24. G. Gunasekaran, L. R. Chauhan, *Electrochim Acta*, 49 (2004) 4387.
25. A. K. Satapathy, G. Gunasekaran, S. C. Sahoo, A. Kumar, P. V. Rodrigues, *Corros. Sci.*, 51 (2009) 2848.
26. P.C. Okafor, M. E. Ikpi, I. E. Uwah, E. E. Ebenso, U.J. Ekpe, S. A. Umoren, *Corros. Sci.*, 50 (2008) 2310.
27. A. Y. El-Etre, *Corros. Sci.,*45 (2003) 2485.
28. A. Bouyanzer, B. Hammouti, L. Majidi, *Mater. Lett.*, 60 (2006) 2840.

29. M. Abdullah, S. O. Al Karanee, A. A. Abdel Fattah, *Chem. Eng. Commun*., 196 (2009) 1406.
30. P. Bothi Raja, M. G. Sethuraman, *Mater. Lett.*, 62 (2009) 2977.
31. M. G. Sethuraman, P. Bothi Raja, *Pigment Res Technol.*, 34 (2005) 327.
32. P. Bothi Raja, M. G. Sethuraman , *Mater. Corros*., 60 (2009) 22.
33. A. Y. El-Etre, *Appl Surf Sci.*, 252 (2006) 8521.
34. A. M. Abdel-Gaber, B. A. Abd-El-Nabey, M. Saadawy, *Corros. Sci*., 51 (2009) 1038.
35. O. K. Abiola, J. O. E. Otaigbe, O. J. Kio, *Corros. Sci*., 51 (2009) 1879.
36. E. E. Oguzie, G. N. Onuoha, E. E. Ejike, *Pigment Res Technol*., 36 (2007) 44.
37. O. K. Abiola, A. O. James, *Corros. Sci*.,52 (2010) 661.
38. A. Saeed , F. A. Larik , P.A. Channar , H. Mehfooz , M. H. Ashraf , Q. Abbas , M. Hassan, S.Y. Seo., *Chem Biol Drug Des.*, 7 (2017) 1.
39. G. N. Mu, T. P. Zhao, M. Liu, T. Gu, *Corrosion*, 52 (1996) 853.
40. R. G. Parr, D. A. Donnelly, M. Levy, M. Palke, *J. Chem. Phys.*, 68 (1978) 3801.
41. A. K. Maayta, N. A. Al-Rawashdeh, *Corros. Sci.*, 46 (2004) 1129.
42. J. Aljourani, K. Raeissi, M. A. Golozar, *Corros. Sci.*, 51 (2009) 1836.
43. H. Amar, A. Tounsi, A. Makayssi, A. Derja, J. Benzakour, A. Outzourhit, *Corros.Sci.*, 49 (2007) 2936.
44. M. A. Migahed, E. M. S. Azzam, S. M. I. Morsy, *Corros.Sci.*, 51 (2009) 1636.
45. M. N.H. Moussa, A. A. El-Far, A. A. El-Shafei, *Mater.Chem.Phys*., 105 (2007) 105.
46. M. Benabdellah, R. Touzan, A. Aouniti, A. S. Dafali, S. El-Kadiri, B. Hommouti, M. Benkaddour, *Mater. Chem. Phys*., 105 (2007) 373.
47. I. Epelboin, M. Keddam, H. Takenouti, *J. Appl. Electrochem*., 2 (1972) 71.
48. J. C. Bessone Mayer, K. Tuttner, W. J. Lorenz, *Electrochim. Acta*, 28 (1983) 171.
49. E. A. Noorand, A. H. Al-Moubaraki, *Mater.Chem.Phys.*, 110 (2008) 145.
50. G. Moretti, G. Quartanone, A. Tassan, A. Zingales, *Wekst. Korros*., 45 (1994) 641.
51. K. Shalabi, Y. M. Abdallah, H. M. Hassan, A. S. Fouda, *Int. J. Electrochem. Sci.*, 9 (2014) 1468.
52. E. Khamis, *Corrosion (NACE)* 46 (1990) 476.
53. A. A. El-Awady, B. Abd El-Nabey, S. G. Aziz, *Electrochem. Soc*., 139 (1992) 2149.
54. J. Lipkowski, P. N. Ross (Eds.) Adsorption of Molecules at Metal Electrodes, *VCH, New York*. (1992).
55. S. L. F. A. Da Costa, S. M. L.Agostinho, *Corrosion*, 46 (1989) 472.
56. E. F. El-Sherbiny, *Mater. Chem. Phys*., 60 (1999) 286.
57. A. S. Fouda, A. A. Al-Sarawy, E. E. El-Katori, *Desalination*, 201 (2006) 1.
58. A. K. Singh, M. A. Quraishi, *Corros. Sci.*, 53 (2012) 1288-1297.
59. R. D. Armstrong, C.A. Hall, *Electrochim. Acta*, 40 (1995) 1135.
60. I. Ahamad, R. Prasad, M. A. Quraishi, *Corros. Sci.*, 52 (2010) 46.
61. G. N. Mu, T.P. Zhao, M. Liu, T. GU, *Corrosion*, 52 (1996*)* 8.